Discrimination Among Non Severe, Severe, and Derecho Mesoscale Convective System Environments

Ariel E. Cohen*
National Weather Center Research Experiences for Undergraduates, Norman, OK
The Ohio State University, Columbus, OH

Michael C. Coniglio
NOAA/OAR/National Severe Storms Laboratory, Norman, OK

Stephen F. Corfidi
NOAA/NWS/NCEP/Storm Prediction Center, Norman, OK

Sarah J. Taylor
NOAA/NWS/NCEP/Storm Prediction Center, Norman, OK

Research Experiences for Undergraduates Final Project
5 August 2005

**Corresponding Author Address:*
Ariel E. Cohen
139 Caren Avenue
Worthington, OH 43085
E-Mail: cohen.274@osu.edu
Phone: 614-841-9153

ABSTRACT

Previous studies have identified meteorological variables linked with intense mesoscale convective systems (MCSs) known as derecho-producing MCSs (DCSs). The prediction of MCS intensity is of concern to operational meteorologists, and this study provides discussion on meteorological variables derived from proximity soundings that can be used to discriminate among DCSs, severe but non derecho-producing MCSs (SCSs), and non severe MCSs (NCSs). These variables have been grouped into three categories: kinematics, instability, and moisture. Two-hundred sixty-nine warm season MCSs were rated based on intensity, and the stage of each system within the typical MCS lifecycle was assessed. Decaying and dissipating MCSs were removed from the data set to focus on the most intense stages of the MCS lifecycle. Variables were calculated from proximity soundings associated with each MCS, and statistical analyses were performed on these calculations. System-relative inflow and mid-level environmental lapse rates were found to be variables that discriminate among all three MCS environments. Knowledge of the variables affecting MCS intensity can allow for improved forecasts and warnings of convective wind events.

1. Introduction

Organized thunderstorms can produce widespread damaging winds responsible for casualties. Organized thunderstorms meeting particular spatial and temporal requirements have been termed mesoscale convective systems (MCSs) (Parker and Johnson 2000). Knowledge of environmental parameters useful in predicting MCS intensity, especially the most intense and long-lasting MCSs known as derecho-producing MCSs (DCSs), is essential in operational meteorology.

One of the first detailed examinations of DCSs was Johns and Hirt (1987), whose work was based on a data set of 70 MCSs occurring during the warm season (May through August of 1980 through 1983). This study discussed the relationship between MCS position, motion, and synoptic scale boundaries. Additionally, Johns and Hirt (1987) found that dry air in mid levels overlaying moist air in low levels was associated with DCS environments. This was found to result in enhanced negative buoyancy in the low levels. The Johns and Hirt (1987) study also found that large negative LIs were associated with DCS environments.

Evans and Doswell (2001) examined 67 DCSs that occurred year-round. As in Johns and Hirt (1987), relatively strong mean flow was linked with DCSs, but Evans and Doswell (2001) also linked low-level and mid-level system relative winds to DCSs. Forcing on the synoptic scale was found to affect the convective available potential energy (CAPE) and wind shear environments, which exhibited high variability among the DCSs studied.

Coniglio et al. (2004) used proximity soundings to determine characteristics of DCS environments during the various stages of a typical DCS's lifecycle, as well as the synoptic-scale forcing patterns that support DCSs. One of the environmental variables considered was the vertical gradient of theta-e (θ_e).

While many features of DCS environments have been discussed in the aforementioned investigations, a study on the variables that discriminate specifically among non severe, severe but non derecho-producing, and derecho-producing MCS environments has not yet been presented. Accordingly, the purpose of the present work is to examaine the meteorological variables derived from proximity soundings that are most likely to predict MCS intensity. Section 2 describes the data set of MCSs considered in this study, as well as the scheme used to rate the MCSs in the data set. Section 3 describes the statistical analyses applied to the data set. Sections 4, 5, and 6 describe the use of the kinematics, instability, and moisture variables, respectively, in MCS environment discrimination. Results are summarized in section 7.

2. MCS Data set and MCS Intensity Rating Scheme

Using archived radar images provided by the University Corporation for Atmospheric Research (UCAR), 269 MCSs were identified for this study. These MCSs were also included in the Coniglio et al. (2005) data set. These MCSs occurred east of the Rocky Mountains during each warm season (May through early September) from 1998 through 2004. Each had an associated proximity sounding from upper air observations. Each proximity sounding was selected so that, within three hours of the time of sounding data collection, the nearest part of the 50 dBz radar reflectivity contour of the MCS was no more than 200 km from the selected sounding. At the time of the proximity sounding, three additional pieces of information about the MCS were also assessed using the radar data: the speed and direction of the leading-line MCS motion, and the stage of the MCS in its lifecycle. The four lifecycle stages used to classify MCSs in this study were (1) initial cells prior to MCS development, (2) mature MCS with strengthening or quasi-steady high reflectivity (50 dBZ or higher), (3) mature MCS with

significantly weakening or shrinking areas of high reflectivity, and (4) the loss of MCS organization and its areas of high reflectivity.

Following the above preliminary work, each MCS was subjectively rated on the basis of intensity. The three categories of intensity considered for each MCS were non severe MCSs (NCSs), severe but non derecho-producing MCSs (SCSs), and derecho-producing MCSs (DCSs). Since this study focuses on the convective systems that produce severe wind, MCS intensity was based solely on severe wind reports. Classification of each MCS required subjectivity, and the criteria used are broad.

The two tools used to classify MCS intensity were national radar images from the UCAR archive and storm reports from the Storm Prediction Center (SPC) data base. For all 269 MCSs, the number and intensity of severe wind reports produced by the MCS were determined using SeverePlot (Hart and Janish 2003). Since SeverePlot did not provide storm reports for 2004 at the time of classification, the "Storm Reports" page from the SPC website (available online: **http://www.spc.noaa.gov/climo**) was used to perform the same classification process.

As mentioned earlier, the intensity classification criteria applied in this study are broad. Several of these criteria, especially for the identification of DCSs, were adapted from the discussion provided in Coniglio et al. (2004). For an MCS to be classified as an SCS or as a DCS, it must have produced at least six severe wind reports. If an MCS did not meet this criterion, then it was classified as an NCS.

Three criteria were used to classify an MCS as a DCS: (1) there were at least 6 severe wind reports produced by the single MCS as recorded in SeverePlot or "Storm Reports," (2) successive severe wind reports occurred within 3 hours or 250 km of each other, and

(3) the major axis length connecting the initial and final severe wind reports was at least 400 km long. If the MCS did not meet these criteria, then it was classified as an SCS.

As mentioned above, "severe wind reports" were used as the basis of MCS intensity. However, not all reports of "severe" convective winds are associated with measured wind gusts greater than or equal to 50 knots (the weakest possible gust speed considered, by National Weather Service definition, to be severe). Therefore, some of the MCSs may have been under- or over-estimated in intensity due to inaccurate reporting and/or a lack of observed severe wind events (see Weiss et al. 2002 for further discussion on problems with the severe convective wind data base). Figure 1 shows sample wind damage and severe wind gust report distributions produced by an NCS, an SCS, and a DCS. These distributions were generated from SeverePlot.

Once the data set was stratified by MCS intensity, it was further classified by the stage of the MCS in its lifecycle. All MCSs that were decaying or dissipating (i.e. within the third and fourth stages of a typical MCS lifecycle mentioned earlier) were removed from the data set to focus on the most intense stages of the MCS lifecycle. This was done so that quantities calculated from the proximity soundings would best represent the MCS when it was most intense.

After the above two stratifications were made, a total of 49 NCSs, 87 SCSs, and 52 DCSs were identified.

3. Statistical Methods

A total of 258 variables were calculated using data collected from proximity soundings associated with each MCS. These variables were grouped into three categories: kinematics, instability, and moisture. This study focuses on the 63 variables that were found to best

discriminate among the three MCS intensities. For each variable, the sample mean, standard deviation, and 99% confidence interval were calculated for each of the three MCS intensities. Figures 2, 4, 6, 8, and 10 show the mean and upper and lower limits of the 99% confidence interval of the three MCS intensities. A table listing a description and unit of measurement used for each of the variables considered is given in Table 1.

Hypothesis testing showed low probabilities (P-Values) that the sample means between any two MCS intensities were the same for several variables. The corresponding absolute values of Z-Scores were also calculated. In this study, absolute values of Z-Scores (P-Values) above 1.645 or 2.33 (below 0.10 or 0.02) are considered to indicate if a variable does a good job or an excellent job, respectively, discriminating between two MCS intensities. Absolute values of Z-Scores and P-Values for each variable are displayed in Figures 3, 5, 7, 9, and 11. In determining the P-Values, it was assumed that the data was distributed in a two-tailed t-distribution. Additionally, when comparing the standard deviation of population means, the standard deviation of any variable was assumed to be the same among the two compared MCS intensities. Z-Scores were calculated from P-Values, and it was assumed that the P-Values are normally distributed.

4. Kinematics variables

Within the mid and upper troposphere, mean winds were found to be excellent discriminators between SCS and DCS environments and between NCS and DCS environments (Figs. 2 and 3). This suggests that downward transport of fast horizontal winds aloft occurs with DCSs and is responsible for a significant part of the damaging surface winds observed.

This study also found that, with increasing MCS intensity, the MCS speed also increased. From Corfidi 2003, increasing mean mid- and upper-level environmental wind speeds were associated with increasing MCS speed. Since mean mid- and upper-level environmental wind speeds were found to be linked with MCS intensity, the link between MCS intensity and MCS speed is consistent.

The angle between the mean wind vector and the MCS motion vector was also studied. For DCSs, this angle exhibited the smallest variability, indicated by the smallest 99% confidence intervals (Figs. 2 and 3). This angle was found to be positive, but near zero, and did an excellent job discriminating between NCSs and DCSs for 0-8 km and 0-10 km mean winds. A positive angle indicates MCS motion to the right of the mean wind vector.

This result supports the technique to determine the net MCS motion vector given in Corfidi (2003). The fast mean winds associated with DCSs yield a strong dominance of the mean wind vector over the propagation vector. It is reasonable that the mean wind vector in several layers of the troposphere and the MCS motion vector would be nearly parallel, with a slight component of the MCS motion vector to the right of the mean wind vector due to cell propagation.

The magnitudes of the wind shear vectors were found to be largest in DCS environments (Figs. 2 and 3). The mean shear in the 0-6 km, 0-8 km, 0-4 km, 4-8 km, and 0-10 km layers was found to discriminate very well between SCS and DCS and between NCS and DCS environments. However, wind shear generally does not do as well discriminating among the MCS environments as does mean wind speed, as indicated by the higher P-Values for wind shear variables.

The effect of wind shear on MCS intensity may be explained by the conceptual model that describes the effects of wind shear on MCSs presented by Weisman et al. (1988). Weisman et al. (1988) described the importance of environmental wind shear in the interaction and development of a cold pool in a strong MCS. Model simulations indicated that wind shear in severe MCS environments is large enough to balance this cold pool. This balance implies generation of upright convective cells, initially, before enough horizontal vorticity generated by the cold pool causes the cells to tilt upwind and a rear-inflow jet to form that descends toward the surface. This rear-inflow jet enhances surface winds. Assuming that this model provides an accurate depiction of the real atmosphere, the results of this study are reasonable, as this study found that MCS intensity increases with increasing shear.

However, the observed values of the environmental wind shear may not be strong enough to balance the cold pool as described above. The model presented in Weisman et al. (1988) assumed that the environmental shear would be large enough to balance the cold pool. In comments made to Weisman and Rotunno (2004) in Stensrud et al. (2004), the large low-level shear values needed to balance the cold pool to produce persistent DCS structures are not found to occur in the atmosphere. Additionally, the cold pool balance suggested by the model is not supported by observational data. Shear exists in a much deeper portion of the real atmosphere compared to the more confined layer used in the modeling studies, which formed the basis of Weisman et al. (1988).

Whether or not the environmental wind shear is strong enough in any MCS environment to balance the cold pool, the cold pool enhances convergence, lift, and convection on its leading edge. These processes can lead to enhanced surface winds.

The increase of shear with increasing MCS intensity may be related to the interaction between shear strength and mean wind speed strength. As mentioned earlier, relatively strong mean winds were found to be linked with DCSs, which may imply that large shear magnitudes may be linked with DCSs (Figs. 2 and 3), as mean winds and wind shear typically are correlated (Evans and Doswell 2001).

This study also found that the angle between the shear and the motion of an MCS is relatively small, but is a good discriminator for the 0-4 km, 0-6 km, and 0-10 km shear vectors (Figs. 4 and 5). Small, nonzero angles were found to exist between the shear vectors in these layers and the MCS motion vector. This indicates that MCSs have a tendency to move at a small angle to the shear vectors in these layers. These results are consistent with observations. MCSs have generally been observed to follow constant thickness lines, with lower thicknesses to the left of the motion (i.e. in the same direction as the thermal wind vector). Since the thermal wind vector is the vertical shear of the horizontal wind vector, one would expect that the angle between the shear and MCS motion vectors would be relatively small, as found in this study. This angle is nonzero due to effect of cell propagation on net MCS motion. The angle was found to be much smaller for DCSs, indicating that DCSs tend to follow the shear vector more closely than SCSs.

The projection of the shear vector onto the MCS motion vector discriminates quite well among MCS environments (Figs. 4 and 5). Additionally, this projection is of similar length to the magnitude of the shear vector. The magnitude of the component of the shear in the direction of the MCS would likely be almost identical to the magnitude of the shear within the same layer. Both the angle between the shear and MCS motion vector, as well as the component of the shear in the direction of the MCS motion vector, may also be associated with other MCS phenomena,

including the way in which hydrometeors are distributed with respect to the motion of the MCS (Parker and Johnson 2000).

Evans and Doswell (2001) identified the importance of system-relative inflow as a discriminator among non DCS and DCS environments, especially within the 0-2-km layer. They attributed this finding to the faster motion of DCSs over non DCSs. In this study, MCS speed was confirmed to increase with increasing inflow speed. In fact, MCS speed was found to be an excellent discriminator among MCS environments. In this study, negative system relative winds indicate inflow. Therefore, mean system-relative inflow was found to increase with increasing MCS speed, and was found to be a good discriminator among all three MCS environments (Figs. 4 and 5), consistent with findings in Evans and Doswell (2001).

The average top of the inflow layer was calculated among each MCS grouping and was also found to discriminate quite well among the MCS environments. The average top of inflow layer was shown to increase as MCS intensity increases (Figs. 4 and 5). The total effect of the system- relative inflow can be found by summing the inflow winds at every level within the inflow layer. Because of the relationship between a thicker inflow layer and MCS intensity, a thicker inflow layer may imply a stronger MCS.

5. Instability variables

Several instability variables do quite well discriminating among the MCS environments (Figs. 6 and 7). Environmental lapse rates within several layers of the troposphere and several variations of CAPE and EL are good discriminators among MCS environments. In fact, of all the groups of variables considered in this study, instability variables appear to be best in discriminating, as their P-Values are lowest, on average.

In this study, the CAPE and EL were determined several different ways. These ways include lifting the surface-based and most unstable parcel, lifting the mixed layer adjacent to the surface, and lifting the most unstable mixed layer. Downdraft CAPE (DCAPE) also was calculated (Gilmore and Wicker 1998).

The EL resulting from the lifting of any parcel or mixed layer was found to be an excellent discriminator among all three categories of MCS environments. Surprisingly, the EL associated with DCSs was found to be lower than that of SCSs but larger than that of NCSs. Lower ELs, on average, were found to be associated with smaller CAPE values.

This study found that CAPE is not a good discriminator between SCS and DCS environments, but is between the other two sets of MCS environments. In fact, average CAPE was found to be smaller in DCS than in SCS environments in some cases. This may be due to the impact of the horizontal distribution of the CAPE relative to the MCS, which would not be reflected in a one-dimensional proximity sounding. A given CAPE distribution may yield a DCS environment, while another CAPE distribution may yield an SCS environment. CAPE may also fail to discriminate well between SCS and DCS environments in this study, because the data set may have included DCSs that could have thrived in strongly forced environments with smaller CAPE, lowering the mean CAPE for DCSs environments.

Evans and Doswell (2001) indicated that DCAPE can be considered as an approximation of the cold pool strength. As mentioned in the kinematics section, the cold pool is responsible for enhanced convergence and convection. Environmental shear enhances the cold pool by separating the updraft from precipitation. It was found that, as environmental shear increases, so does MCS intensity, and thus cold pool strength. This is consistent with finding increasing

DCAPE with increasing MCS intensity. In fact, DCAPE was found to be a very good discriminator among the MCS environments.

Tropospheric environmental lapse rates also describe instability. Despite CAPE being larger for SCSs than for DCSs and NCSs, the environmental lapse rate was found to be largest for DCSs in the 2-4 km, 4-6 km, and 6-8 km layers (Figs. 8 and 9). The 4-6 km and 4-8 km environmental lapse rates both discriminate among all three MCS environments with P-Values below 0.10, especially between SCS and DCS environments. While the CAPE associated with DCSs was found to be relatively smaller than that associated with SCSs, the environmental lapse rate was found to be largest in DCS environments. Because the environmental lapse rate is not an integrated quantity, as is CAPE, environmental lapse rate is more likely to uncover some small-scale instability features in the vertical masked by CAPE. So, in measuring instability, mid-level environmental lapse rates may generally be better discriminators than CAPE. However, as with CAPE, the horizontal distribution of the environmental lapse rate may also affect MCS intensity, which cannot be determined by a proximity sounding.

6. Moisture variables

Theat-e (θ_e) is a measure of moisture. A vertical gradient in θ_e with height was considered in this study. A positive vertical gradient in θ_e means that θ_e increases with height, and a negative vertical gradient means that θ_e decreases with height (Figs. 10 and 11). Coniglio et al. (2004) found that MCSs were generally weakening where the vertical gradient in θ_e was relatively smaller, although not significantly. In this study, a vertical gradient in θ_e with height was found to be an excellent discriminator between NCS and SCS environments. This was especially the case for the near-surface to mid-level gradients. The gradient was found to be

least negative for NCSs and generally most negative for SCSs and DCSs, which indicates that θ_e falls more rapidly with height in SCS and DCS environments than in NCS environments.

Therefore, a vertical gradient of θ_e is likely linked with any wind damage potential, and may depend on entrainment in mid-levels, as indicated in Wakimoto (2001). The dry air at mid levels, marked by relatively low θ_e values, leads to entrainment of dry air into the downdraft. This causes a relative increase in downdraft density, since the density of dry air is larger than the density of moist air. This dry air entrainment helps generate evaporational cooling, which helps enhance the negative buoyancy of the downdraft at mid levels. Then, with a relatively moist and less dense environment at low levels, marked by a higher θ_e, the relative density difference between the descending parcel and its environment is enhanced. In MCSs with nearly saturated thermodynamic profiles throughout the entire troposphere, θ_e varies much less with height producing a lower gradient in θ_e. In these nearly saturated profiles, the processes of entraining the denser, drier air and the resulting evaporational cooling would occur relatively less, and downdrafts would be weaker.

The precipitable water (PWAT) was calculated and was found to be a very good discriminator between SCS and DCS environments. The PWAT was found to be smaller in DCS than in SCS environments. As mentioned above, a vertical gradient in θ_e, representing dry mid levels overlaying moist low levels, was found to be important for an enhanced downdraft. If the above description of downdraft enhancing truly applies in the real atmosphere, then a large negative vertical gradient in θ_e would be usually more associated with DCS environments than SCS environments. This would not necessarily be apparent from the layers of vertical gradient of θ_e considered in this study. With drier mid levels in DCS than in SCS environments, larger negative gradients exist in DCS environments than in SCS environments. So, PWAT, which

involves the integration of moisture throughout the depth of the atmosphere, would be lower in DCS environments than in SCS environments. This is consistent with the results in this study that PWAT discriminates well between DCS and SCS environments.

7. Conclusions

This study provided discussion of several meteorological variables that can be used to discriminate among MCS environments. The three MCS environments considered were non severe MCS (NCS), severe but non derecho-producing MCS (SCS), and derecho-producing MCS (DCS) environments. Variables that increase with increasing MCS intensity and that are very good discriminators include mid-level environmental lapse rates, mean mid- and upper-level winds, and deep-layer wind shear. This study also showed that CAPE discriminates well between NCS and SCS environments and between NCS and DCS environments, but not between SCS and DCS environments. The horizontal distribution of CAPE may discriminate between these SCS and DCS environments.

Relationships studied in two papers, Corfidi (2003) and Evans and Doswell (2001) were also explored in this study, and several of their results were verified. For example, Corfidi (2003) suggested adding the advective component of motion, represented by the mean cloud-layer wind, twice to the propagation vector to get net MCS motion. This seems reasonable to do, since MCS motion was found to increase with increasing MCS intensity, just as mean wind speed did. It was also found in this study that there exists a relationship between EL and CAPE and that, in some cases, EL height better discriminates among MCS environments than does CAPE. System-relative inflow was also found to be important in this study, as was found by

Evans and Doswell (2001), and this variable was found to be an excellent discriminator among MCS environments.

This study provided a description of the environments favoring MCS severity based on the analysis of numerous variables and how these variables change specifically in the vertical. This, itself, gives a clearer understanding of the vertical structure of the atmosphere and the way that structure relates to MCS intensity. Combined with an understanding on how the horizontal distribution of these variables affects MCS intensity, one can gain a more complete understanding of the factors contributing to MCS intensity.

Acknowledgements

This material is based on work supported by the National Science Foundation under Grant No. 0097651.

The authors thank the personnel of the National Severe Storms Laboratory (NSSL) and the Storm Prediction Center (SPC) for their help with this project. The authors would also like to thank David Bright (SPC) for his assistance in preparing computer accounts for this work. We greatly appreciate the review of this paper by Dr. Harold Brooks (NSSL). Finally, the authors thank Daphne Zaras for her enormous efforts in running the National Weather Center Research Experiences for Undergraduates program.

Table 1

List of Variables, Their Meanings, and Units

"A-B km" denotes the layer bounded by the A-km level and the B-km level.

Symbol	Explanation	Units
A-B km γ	A - B km environmental lapse rate	°C km^{-1}
SB-CAPE	surface-based convective available potential energy (CAPE)	J kg^{-1}
SB-EL	equilibrium level for the surface-based parcel	m
MU-CAPE	most-unstable CAPE	J kg^{-1}
MU-EL	equilibrium level for the most unstable parcel	m
50 hPa ML-CAPE	lowest 50-hPa mixed layer CAPE	J kg^{-1}
50 hPa ML-EL	equilibrium level for the parcel mixed in the lowest 50-hPa	m
100 hPa ML-CAPE	lowest 100-hPa mixed layer CAPE	J kg^{-1}
100 hPa ML-EL	equilibrium level for the parcel mixed in the lowest 100-hPa	m
150 hPa ML-CAPE	lowest 150-hPa mixed layer CAPE	J kg^{-1}
150 hPa ML-EL	equilibrium level for the parcel mixed in the lowest 150-hPa	m
50 hPa MUML-CAPE	most-unstable 50-hPa mixed layer of the lowest 400 hPa CAPE	J kg^{-1}
50 hPa MUML-EL	equilibrium level for the parcel in the most unstable 50-hPa mixed layer of the lowest 400 hPa	m
100 hPa MUML-CAPE	most-unstable 100-hPa mixed layer of the lowest 400 hPa CAPE	J kg^{-1}
100 hPa MUML-EL	equilibrium level for the parcel in the most unstable 100-hPa mixed layer of the lowest 400 hPa	m
150 hPa MUML-CAPE	most-unstable 150-hPa mixed layer of the lowest 400 hPa CAPE	J kg^{-1}
150 hPa MUML-EL	equilibrium level for the parcel in the most unstable 150-hPa mixed layer of the lowest 400 hPa	m
A-B km $\Delta RH/\Delta z$	A - B km vertical gradient in relative humidity	% km^{-1}
A-B km $\Delta\theta_e/\Delta z$	A - B km vertical gradient in equivalent potential temperature	°C km^{-1}
PWAT	precipitable water	in
A-B km $\lvert\vec{V}\rvert$	A-B km velocity vector measured in the reference frame of the proximity sounding vector magnitude	m s^{-1}
A-B km $\lvert\Delta\vec{V}\rvert$	A-B km wind shear vector magnitude	m s^{-1}
A - B km $\Delta\vec{V}$ comp	component of A-B km $\Delta\vec{V}$ in the direction of the MCS motion vector	m s^{-1}
A-B km α	angle between MCS motion vector and A - B km $\lvert\vec{V}\rvert$ measured counterclockwise from the MCS motion vector	degrees
A-B km β	angle between MCS motion vector and A - B km $\lvert\Delta\vec{V}\rvert$	degrees
ILT	height of the inflow layer top	km
MIW	mean inflow winds in the inflow layer	m s^{-1}

References

Corfidi, S. F., 2003. Cold pools and MCS propagation: Forecasting the motion of downwind-developing MCSs. *Wea. Forecasting*, **18**, 997-1017.

Coniglio, M. C., D. J. Stensrud, and M. B. Richman, 2004. An observational study of derecho-producing convective systems. *Wea. Forecasting*, **19**, 320-337.

Coniglio, M. C., H. E. Brooks, and S. J. Weiss, 2005: Use of proximity sounding parameters to improve the prediction of mesoscale convective system (MCS) speed and dissipation. Preprints, *21st Conf. on Weather Analysis and Forecasting/17th Conference on Numerical Weather Prediction.* Washington, D.C., Amer. Meteor. Soc., 3.3.

Evans, J. S., and C. A. Doswell III, 2001. Examination of Derecho Environments Using Proximity Soundings. *Wea. Forecasting*, **16**, 329-342.

Gilmore M. S., and L. J. Wicker, 1998: The influence of midtropospheric dryness on supercell morphology and evolution. *Mon. Wea. Rev*., **126**, 943-958.

Hart, J. and P. Janish, 2003: SeverePlot v2.2. Historical severe weather report data base. National Weather Service Storm Prediction Center, Norman, Oklahoma. [Available Online: http://www.spc.noaa.gov/software/svrplot2/.]

Image Archive, 2004. *University Corporation for Atmospheric Research.* [Available Online: http://locust.mmm.ucar.edu/case-selection/.]

Johns, R. H., and W. D. Hirt, 1987. Derechos: Widespread Convectively Induced Windstorms. *Wea. Forecasting*, **2**, 32-48.

Parker, M. D., and R. H. Johnson, 2000: Organizational modes of midlatitude mesoscale convective systems. *Mon. Wea. Rev.*, **128,** 3413-3436.

Stensrud, D. J., et al., 2004 : Comments on “A theory for strong long-lived squall lines” revisited. *J. Atmos. Sci.,* in press.

Storm Reports. *Storm Prediction Center.* [Available Online: http://www.spc.noaa.gov/climo/.]

Weisman, M.L., J.B. Klemp, and R. Rotunno, 1988: Structure and evolution of numerically simulated squall lines. *J. Atmos. Sci.,* **45**, 1990-2013.

Weisman, M. L., and R. Rotunno, 2004: “A Theory for long-lived squall lines” revisited. *J. Atmos. Sci.,* **61,** 361-382.

Weiss, S. J., J. A. Hart, and P. R. Janish, 2002: An examination of severe thunderstorm wind report climatology: 1970-1999. Preprints, *21st Conf. on Severe Local Storms,* San Antonio, TX, Amer. Meteor. Soc., 446-449.

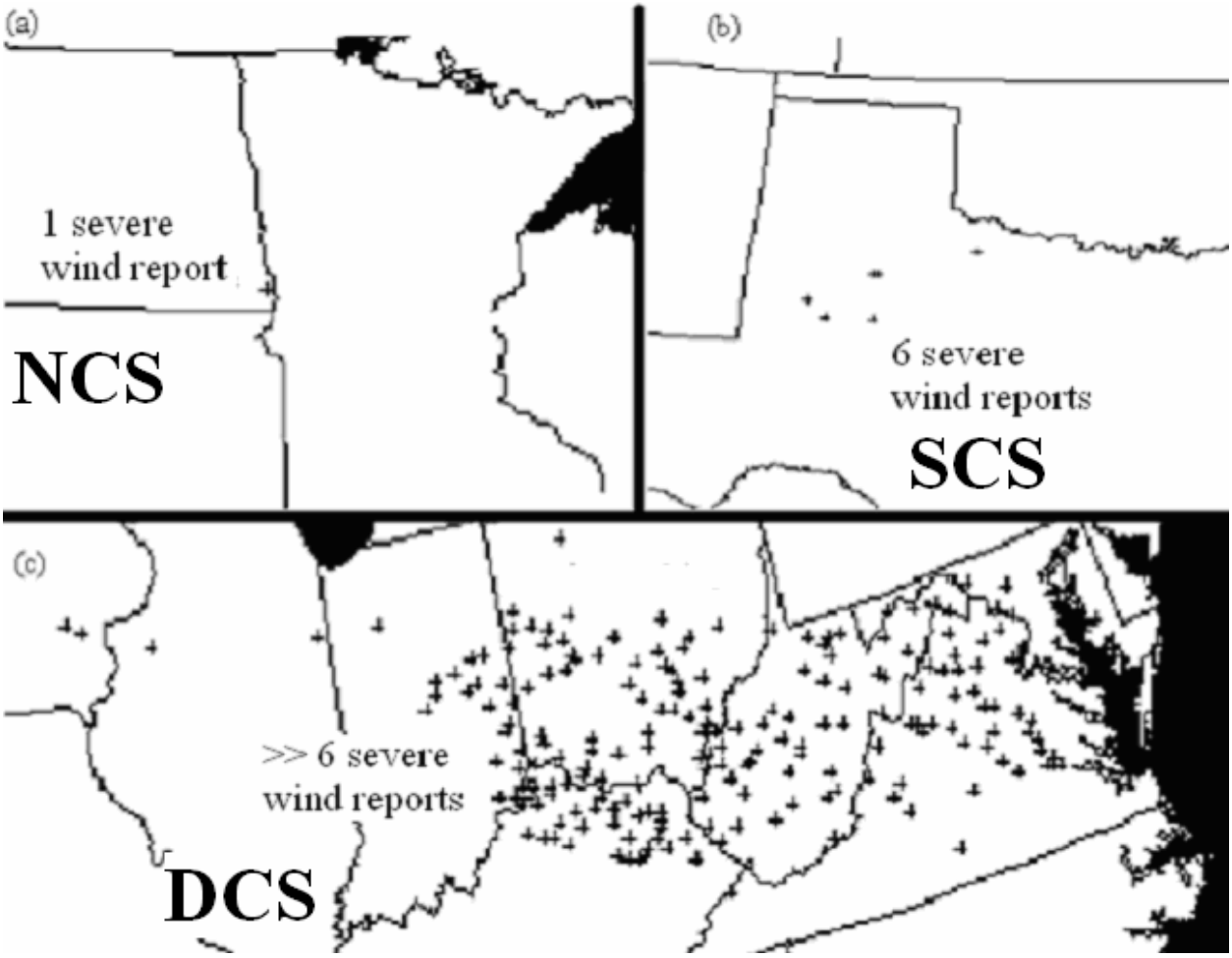

FIG. 1. (a) Wind damage and severe wind gust report distributions associated with an NCS, (b) an SCS, and (c) a DCS.

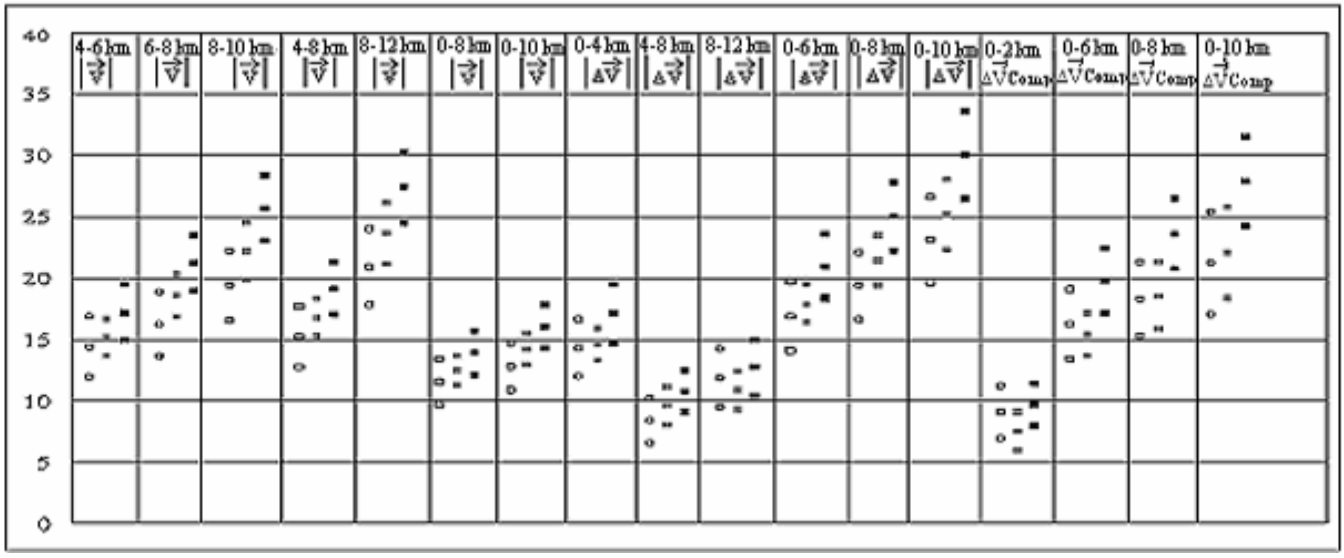

FIG 2. Means and upper and lower bounds on the 99% confidence interval shown by small white, grey, and black squares, respectively, for NCSs, SCSs, and DCSs for kinematics variables in several layers of the atmosphere.

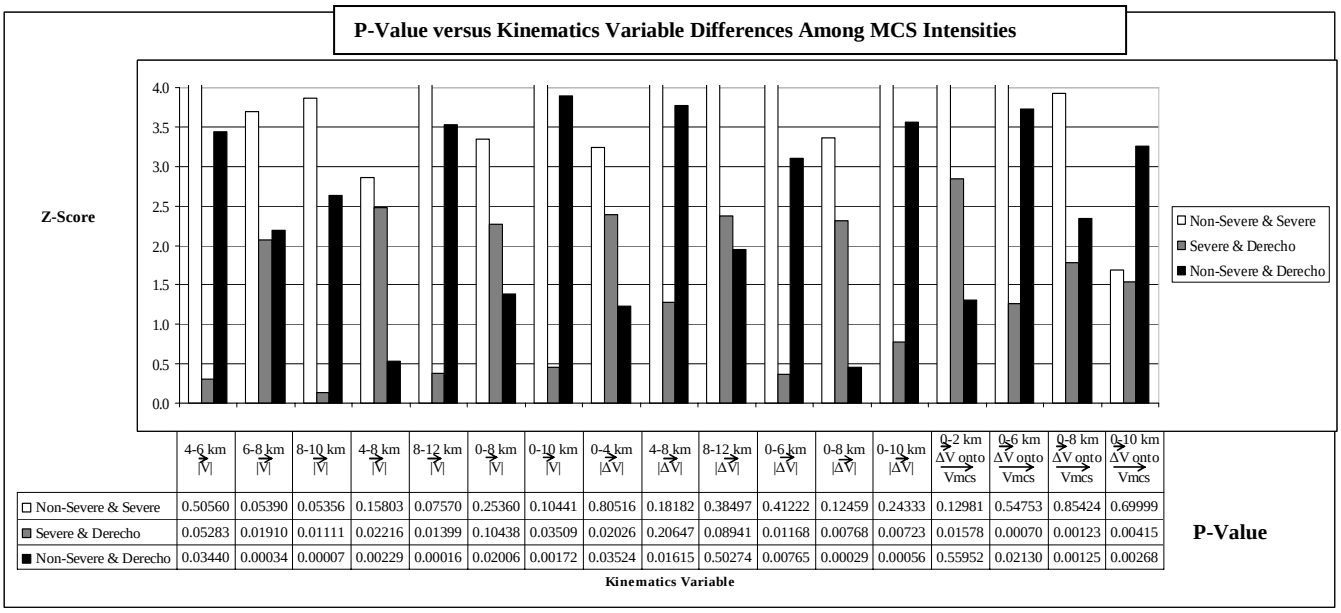

	4-6 km $\vec{V}$	6-8 km $\vec{V}$	8-10 km $\vec{V}$	4-8 km $\vec{V}$	8-12 km $\vec{V}$	0-8 km $\vec{V}$	0-10 km $\vec{V}$	0-4 km $\vec{\Delta V}$	4-8 km $\vec{\Delta V}$	8-12 km $\vec{\Delta V}$	0-6 km $\vec{\Delta V}$	0-8 km $\vec{\Delta V}$	0-10 km $\vec{\Delta V}$	0-2 km $\vec{\Delta V}$ onto Vmcs	0-6 km $\vec{\Delta V}$ onto Vmcs	0-8 km $\vec{\Delta V}$ onto Vmcs	0-10 km $\vec{\Delta V}$ onto Vmcs
Non-Severe & Severe	0.50560	0.05390	0.05356	0.15803	0.07570	0.25360	0.10441	0.80516	0.18182	0.38497	0.41222	0.12459	0.24333	0.12981	0.54753	0.85424	0.69999
Severe & Derecho	0.05283	0.01910	0.01111	0.02216	0.01399	0.10438	0.03509	0.02026	0.20647	0.08941	0.01168	0.00768	0.00723	0.01578	0.00070	0.00123	0.00415
Non-Severe & Derecho	0.03440	0.00034	0.00007	0.00229	0.00016	0.02006	0.00172	0.03524	0.01615	0.50274	0.00765	0.00029	0.00056	0.55952	0.02130	0.00125	0.00268

FIG 3. Absolute values of Z-Scores and P-Values resulting from hypothesis testing shown by white, grey, and black bars, respectively, between NCSs and SCSs, SCSs and DCSs, and NCSs and DCSs for kinematics variables in several layers of the atmosphere.

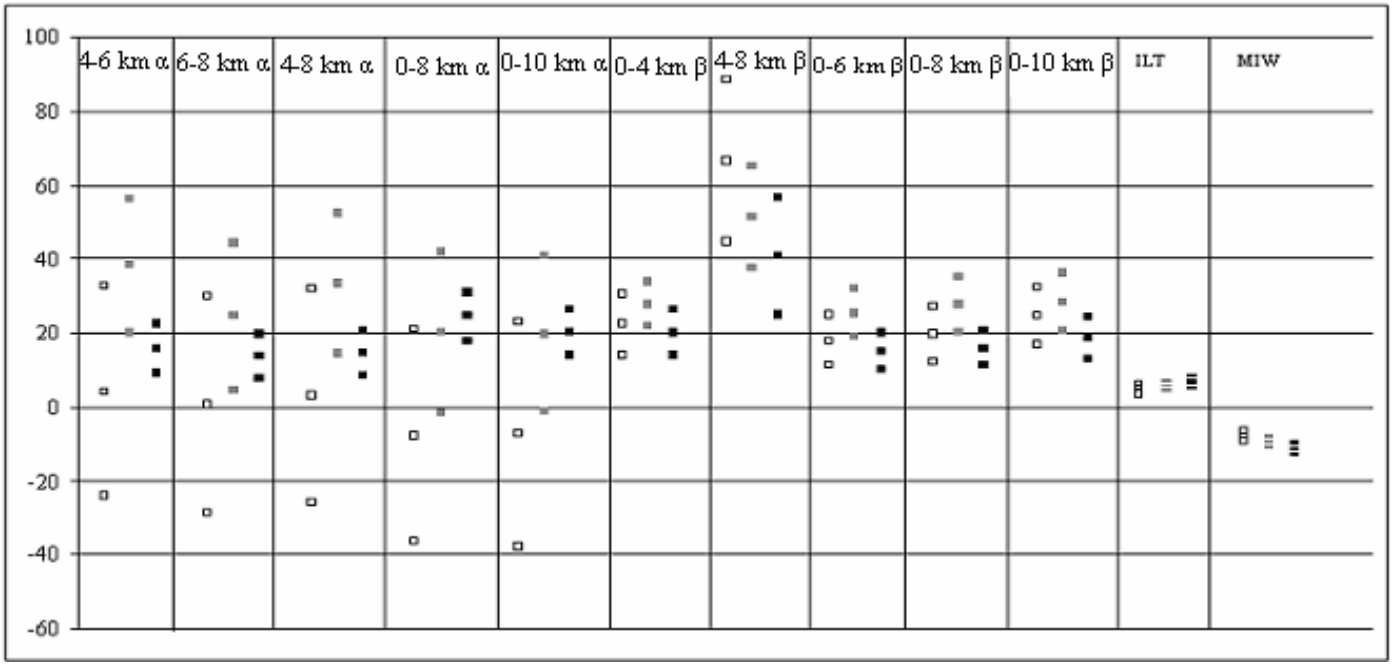

FIG 4. Same as in Fig. 2, except for kinematics angle and inflow variables.

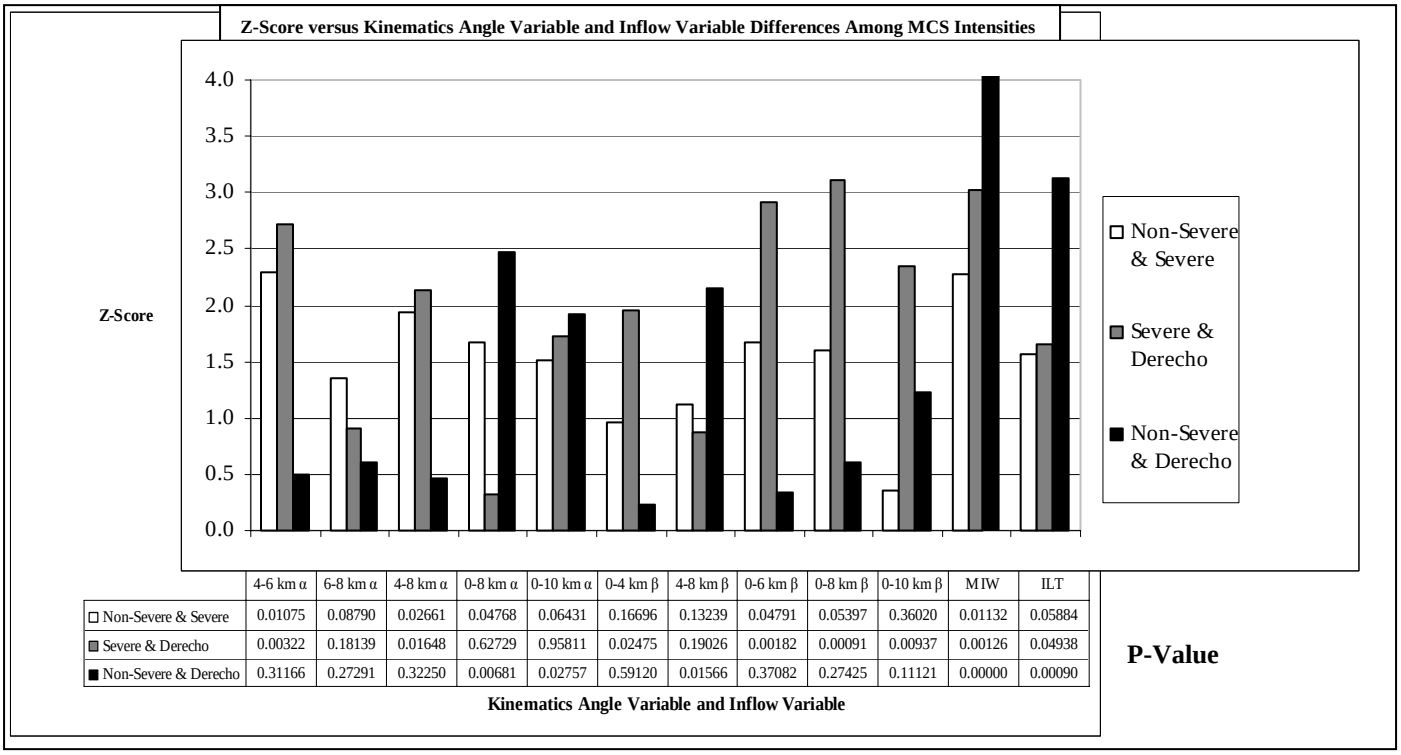

	4-6 km α	6-8 km α	4-8 km α	0-8 km α	0-10 km α	0-4 km β	4-8 km β	0-6 km β	0-8 km β	0-10 km β	MIW	ILT
Non-Severe & Severe	0.01075	0.08790	0.02661	0.04768	0.06431	0.16696	0.13239	0.04791	0.05397	0.36020	0.01132	0.05884
Severe & Derecho	0.00322	0.18139	0.01648	0.62729	0.95811	0.02475	0.19026	0.00182	0.00091	0.00937	0.00126	0.04938
Non-Severe & Derecho	0.31166	0.27291	0.32250	0.00681	0.02757	0.59120	0.01566	0.37082	0.27425	0.11121	0.00000	0.00090

P-Value

FIG 5. Same as in Fig. 3, except for kinematics angle and inflow variables.

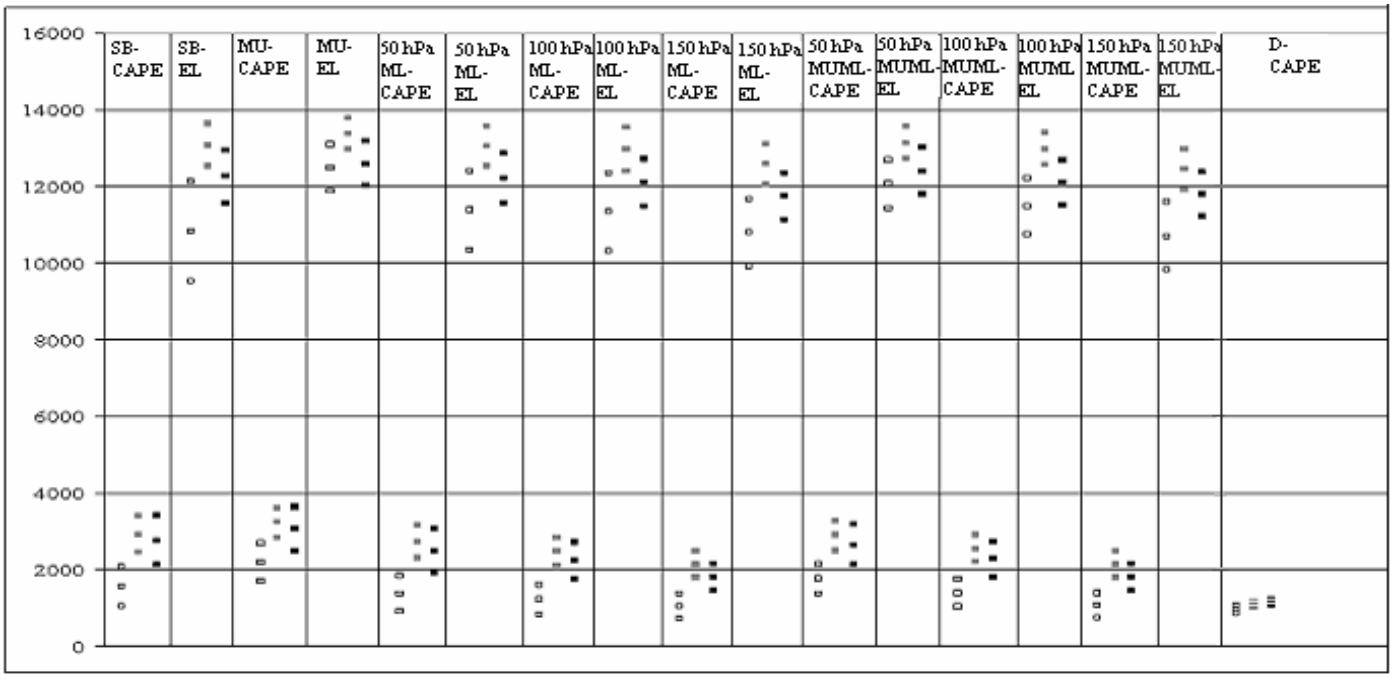

FIG 6. Same as in Fig. 2, except for CAPE and EL variables.

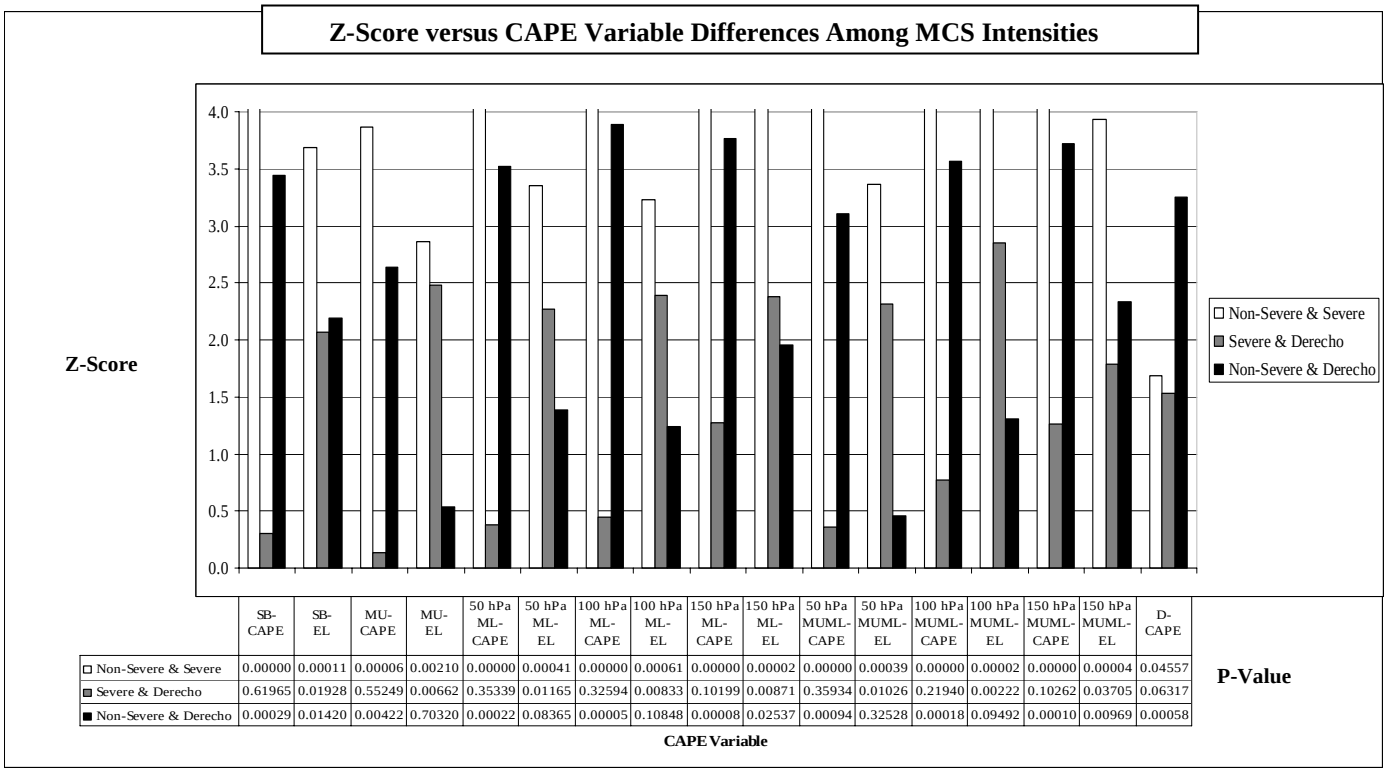

	SB-CAPE	SB-EL	MU-CAPE	MU-EL	50 hPa ML-CAPE	50 hPa ML-EL	100 hPa ML-CAPE	100 hPa ML-EL	150 hPa ML-CAPE	150 hPa ML-EL	50 hPa MUML-CAPE	50 hPa MUML-EL	100 hPa MUML-CAPE	100 hPa MUML-EL	150 hPa MUML-CAPE	150 hPa MUML-EL	D-CAPE
□ Non-Severe & Severe	0.00000	0.00011	0.00006	0.00210	0.00000	0.00041	0.00000	0.00061	0.00000	0.00002	0.00000	0.00039	0.00000	0.00002	0.00000	0.00004	0.04557
▒ Severe & Derecho	0.61965	0.01928	0.55249	0.00662	0.35339	0.01165	0.32594	0.00833	0.10199	0.00871	0.35934	0.01026	0.21940	0.00222	0.10262	0.03705	0.06317
■ Non-Severe & Derecho	0.00029	0.01420	0.00422	0.70320	0.00022	0.08365	0.00005	0.10848	0.00008	0.02537	0.00094	0.32528	0.00018	0.09492	0.00010	0.00969	0.00058

FIG 7. Same as in Fig. 3 except for CAPE and EL variables.

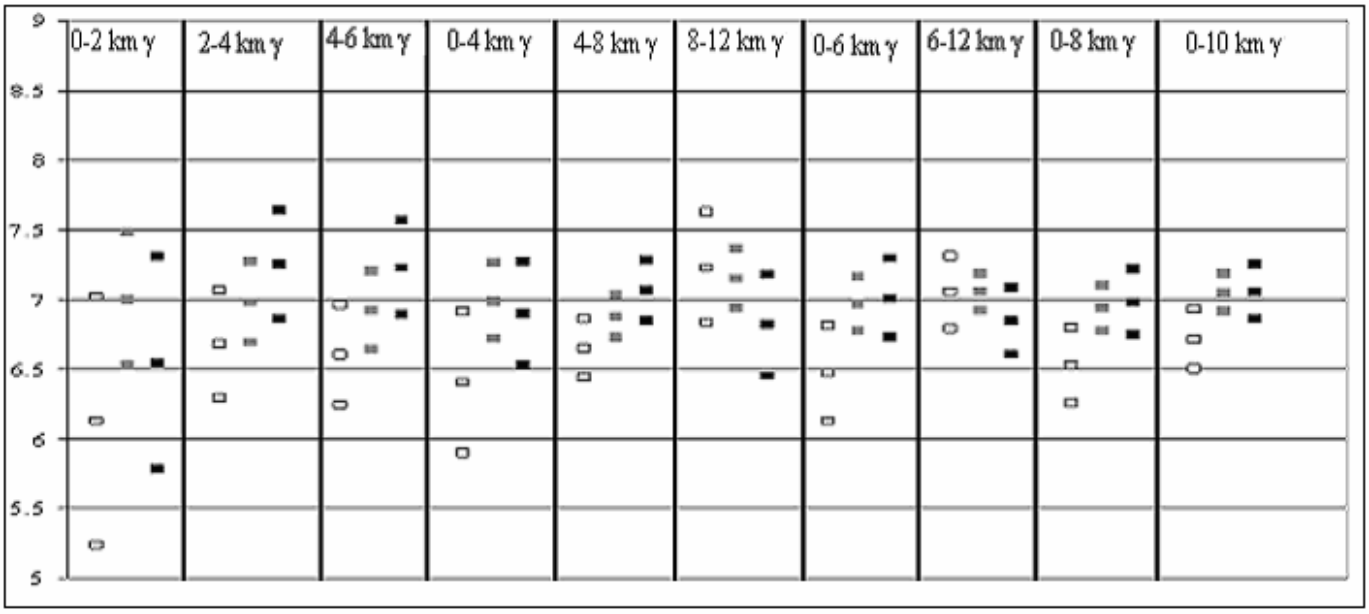

FIG 8. Same as in Fig. 2, except for environmental lapse rate variables.

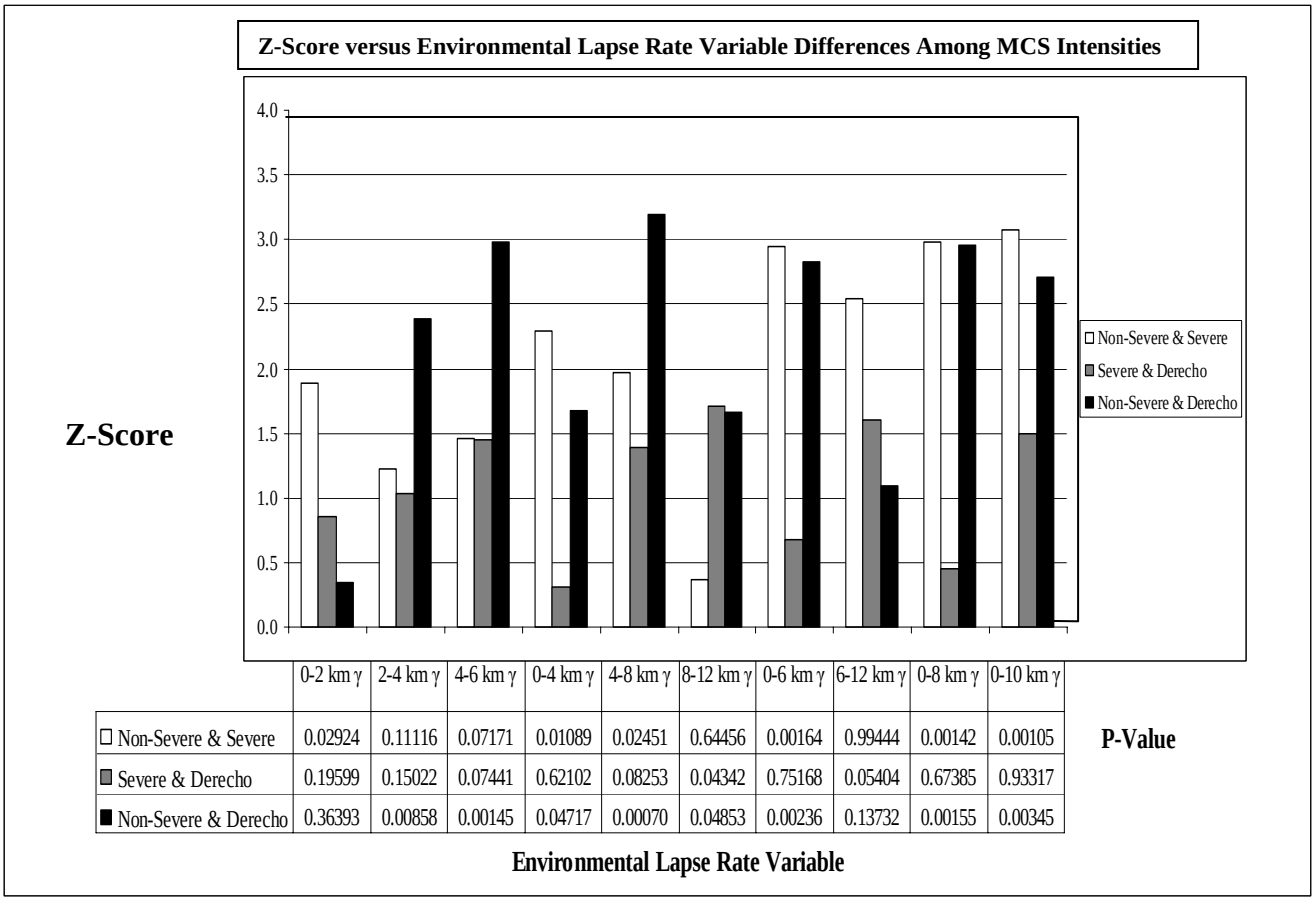

	0-2 km γ	2-4 km γ	4-6 km γ	0-4 km γ	4-8 km γ	8-12 km γ	0-6 km γ	6-12 km γ	0-8 km γ	0-10 km γ
Non-Severe & Severe	0.02924	0.11116	0.07171	0.01089	0.02451	0.64456	0.00164	0.99444	0.00142	0.00105
Severe & Derecho	0.19599	0.15022	0.07441	0.62102	0.08253	0.04342	0.75168	0.05404	0.67385	0.93317
Non-Severe & Derecho	0.36393	0.00858	0.00145	0.04717	0.00070	0.04853	0.00236	0.13732	0.00155	0.00345

FIG 9. Same as in Fig. 3, except for environmental lapse rate variables.

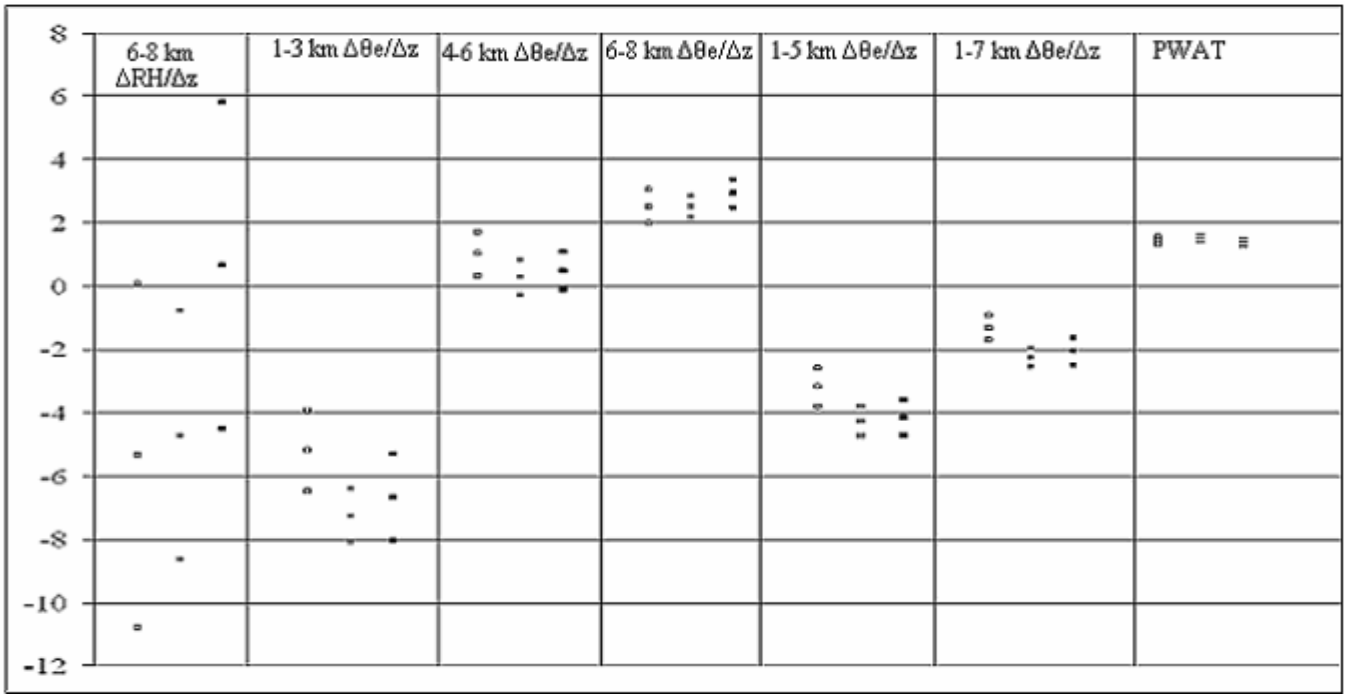

FIG 10. Same as in Fig. 2, except for moisture variables.

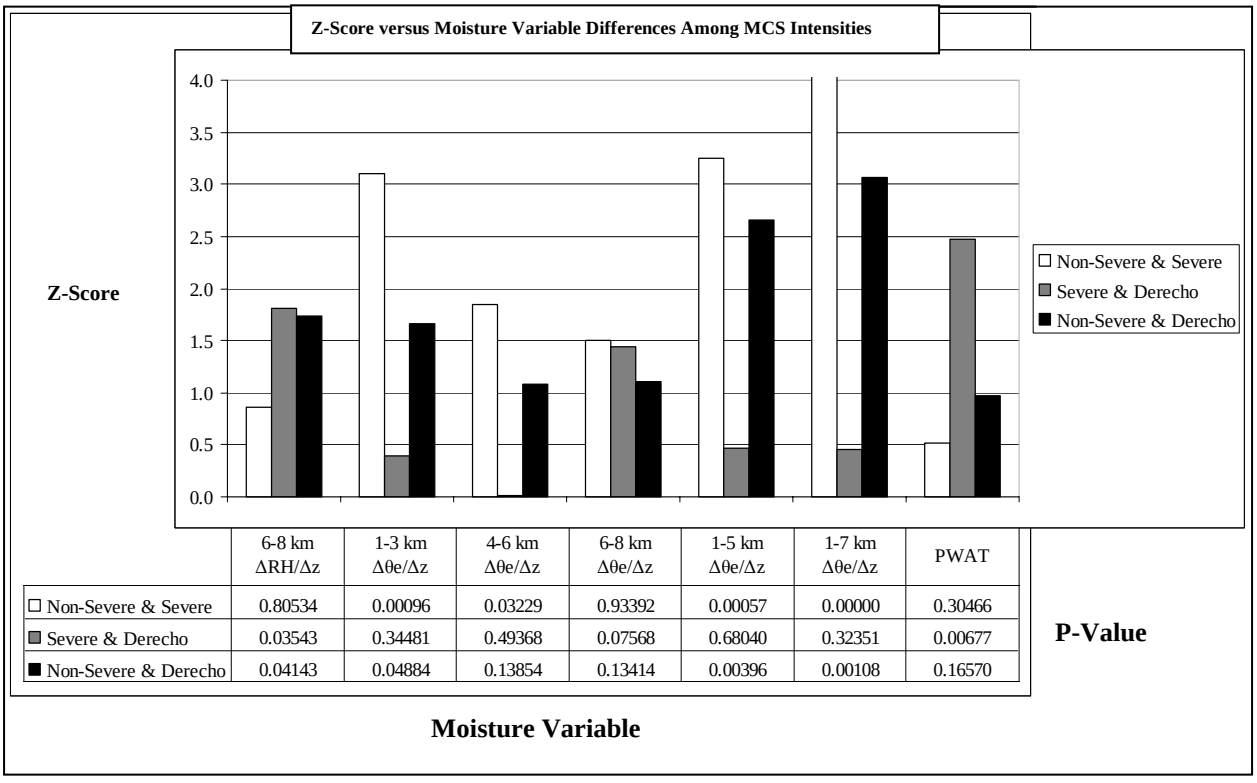

	6-8 km ΔRH/Δz	1-3 km Δθe/Δz	4-6 km Δθe/Δz	6-8 km Δθe/Δz	1-5 km Δθe/Δz	1-7 km Δθe/Δz	PWAT
Non-Severe & Severe	0.80534	0.00096	0.03229	0.93392	0.00057	0.00000	0.30466
Severe & Derecho	0.03543	0.34481	0.49368	0.07568	0.68040	0.32351	0.00677
Non-Severe & Derecho	0.04143	0.04884	0.13854	0.13414	0.00396	0.00108	0.16570

FIG 11. Same as in Fig. 3, except for moisture variables.